Dynamic Modeling and Simulation of a Wheeled Mobile Robot for Traversing Uneven Terrain Without Slip

Nilanjan Chakraborty

Ashitava Ghosal[1]
e-mail: asitava@mecheng.iisc.ernet.in

Department of Mechanical Engineering, Indian Institute of Science, Bangalore, Karnataka 560012, India

It is known in literature that a wheeled mobile robot (WMR), with fixed length axle, will undergo slip when it negotiates an uneven terrain. However, motion without slip is desired in WMR's, since slip at the wheel-ground contact may result in significant wastage of energy and may lead to a larger burden on sensor based navigation algorithms. To avoid slip, the use of a variable length axle (VLA) has been proposed in the literature and the kinematics of the vehicle has been solved depicting no-slip motion. However, the dynamic issues have not been addressed adequately and it is not clear if the VLA concept will work when gravity and inertial loads are taken into account. To achieve slip-free motion on uneven terrain, we have proposed a three-wheeled WMR architecture with torus shaped wheels, and the two rear wheels having lateral tilt capability. The direct and inverse kinematics problem of this WMR has been solved earlier and it was shown by simulation that such a WMR can travel on uneven terrain without slip. In this paper, we derive a set of 27 ordinary differential equations (ODE's) which form the dynamic model of the three-wheeled WMR. The dynamic equations of motion have been derived symbolically using a Lagrangian approach and computer algebra. The holonomic and nonholonomic constraints of constant length and no-slip, respectively, are taken into account in the model. Simulation results clearly show that the three-wheeled WMR can achieve no-slip motion even when dynamic effects are taken into consideration.
[DOI: 10.1115/1.1867503]

1 Introduction

It is a well known fact that for wheeled mobile robots moving on uneven terrain, in general, there is slip at the wheel-terrain contact points. This is because, on uneven terrain there is no unique axis of vehicle rotation that is compatible with all wheel contacts [1]. This is the principal reason that prevents us from applying the techniques used for kinematic analysis of WMR's moving on flat terrain [2,3] to WMR's moving on uneven terrain. The two main problems with slipping of WMR's on uneven terrain are: (a) most autonomous WMR's use odometry to localize their positions during navigation and slip at the wheel-ground contact points leads to accumulation in localization error, and (b) slipping leads to large wastage of power which is at a premium in missions like planetary exploration. The prevention of slip is still an open question, and in this paper, we propose a novel WMR architecture and show by analysis and simulations that the proposed WMR can negotiate uneven terrain without slipping.

There has been a variety of WMR architectures proposed for WMR's on uneven terrain [4–6]. These WMR's are all capable of adapting on uneven terrain but not capable of slip free motion. The problem of slipping of WMR's on uneven terrain has been studied by Sreenivasan et al. [7–9]. The researchers have proposed the use of variable length axle (VLA) and performed kinematic analysis to demonstrate no-slip motion capability [7] with VLA. However, there are a few limitations of using a VLA (a) at high inclinations there is slipping due to gravity loading, and (b) the dynamic slip due to inertial loading becomes large at higher speeds. To overcome the limitations in VLA, the use of an actuated VLA has been proposed. An actuated VLA, however, requires accurate measurement of slip to obtain the desired actuator output. Choi and Sreenivasan [10] have noted that the problem of slip is essentially kinematic in nature and the use of redundant actuation without paying attention to the kinematic design of the vehicle is an unlikely solution to the problem.

It may be noted that one important feature of all the above mentioned work is that they model the wheel as a thin (rigid) disk. On a flat ground this is reasonable since the contact point always lies in a vertical plane passing through the center of the wheel. However, on uneven terrain this is not the case in general and the contact point may vary along the lateral surface of the wheel due to terrain geometry variations. In this paper, we use *torus shaped wheels* in single point contact with an arbitrary terrain, modeled as a *smooth* and (at the least) C^3 continuous surface, and connected to the vehicle body by a *passive* rotary joint allowing lateral tilting of the wheel. This concept possess some similarity to the active camber control [11–13] proposed in the automobile industry. In active camber control, the wheels are allowed to tilt and a special tire profile is used to increase the friction between tire and road. Active camber control helps in prevention of skidding at sharp corners and reduction of stopping distance at high speeds. However, an important distinction is that the tilting of the tires is actively controlled, where as in our case the lateral tilting mechanism is passive. The architecture of the three-wheeled WMR with torus shaped wheels and passive joint for lateral tilting was presented in [14,15], and the direct and inverse kinematic analysis was performed to demonstrate slip-free motion capability on uneven terrain. However, no-slip motion may not be possible if the effects of gravity and inertial forces are considered, and it is imperative to perform a dynamic analysis to demonstrate the no-slip motion capability of the WMR. Moreover, the availability of a dynamic model of the WMR is helpful to design and implement advanced model-based control techniques.

In WMR literature, most of the dynamic analysis on uneven

[1]To whom correspondence should be addressed.

Contributed by the Mechanisms and Robotics Committee for publication in the JOURNAL OF MECHANICAL DESIGN. Manuscript received February 28, 2004; revised October 13, 2004. Associate Editor: M. Raghavan.

terrain is essentially quasi-static in nature, where gravity is taken into account but inertial effects are ignored (see, for example, [16]). In this paper, we use a Lagrangian formulation for multibody systems subjected to holonomic and nonholonomic constraints [17] and derive the equations of motion of the WMR. As mentioned above, we have used a torus as a model for the wheels of the mobile robot. Although the motion of a disk on a plane is a standard textbook problem in dynamics, to the best of our knowledge, the equations of motion of a toroidal wheel moving on uneven terrain has not been reported. Therefore, we first present the derivation of the equations of motion of a toroidal wheel moving with single point contact on an uneven terrain. The approach for a single toroidal wheel is extended to the three-wheeled WMR. The dynamic equations of motion are derived symbolically as a set of 27 second-order ODE's subjected to 21 nonholonomic and 3 holonomic constraints. The derivation of the dynamic model, simulation results and demonstration of no-slip motion when the wheels are subjected to driving and steering torques are the main contributions of this paper.

This paper is organized as follows: In the next section, we present a brief overview of the Lagrangian method of derivation of the equations of motion for a multibody system subject to holonomic and nonholonomic constraints. Then, we present the derivation of the equations of motion of a single wheel moving on uneven terrain. Thereafter, we derive the equations of motion for the three-wheeled robot. The simulation results are provided next to demonstrate no-slip capability of the WMR. Lastly, we present our conclusions and identify the areas of future work.

2 Equations of Motion of a Single Toroidal Wheel

In this section, we derive the equations of motion of a single wheel moving on uneven terrain. First, we give a brief review of the Lagrangian formulation of a system subjected to holonomic and nonholonomic constraints.

Let KE denote the kinetic energy and PE denote the potential energy of the system under consideration. Then the Lagrangian ($\mathcal{L}$) is given by,

$$\mathcal{L} = \mathrm{KE} - \mathrm{PE} \tag{1}$$

The Lagrange's equations of motion are given by,

$$\frac{d}{dt}\left(\frac{\partial \mathcal{L}}{\partial \dot{q}_i}\right) - \frac{\partial \mathcal{L}}{\partial q_i} = Q_i + \tau_i \tag{2}$$

where,

- q_i = generalized coordinates, $i=1,\ldots,n$
- Q_i = component of generalized force acting along the ith coordinate
  = $\mathbf{F}\cdot\partial\mathbf{V}_i/\partial\dot{q}_i + \mathbf{M}\cdot\partial\omega_i/\partial\dot{q}_i$
- $\mathbf{V}_i, \omega_i$ = linear and angular velocities
- $\mathbf{F}$ = force sacting on the body
- $\mathbf{M}$ = moments acting on the body
- τ_i = component of constraint force, τ, acting along the ith coordinate
- τ = $[\mathbf{\Psi}]^T\lambda$
- $[\mathbf{\Psi}]$ = constraint matrix
- λ = Lagrange multipliers

When the number of generalized coordinates are equal to the number of degrees of freedom of the system, $\tau_i=0$, and Eq. (2) reduces to the Euler–Lagrange equations of motion for unconstrained systems. In the case holonomic constraints are present, they are differentiated to obtain

$$[\mathbf{\Psi}]\dot{\mathbf{q}} = \mathbf{0} \tag{3}$$

which gives the required $[\mathbf{\Psi}]$ matrix. For nonholonomic constraints, the constraints are directly available in terms of the first derivatives of generalized coordinates and they are rearranged to be expressed in the form

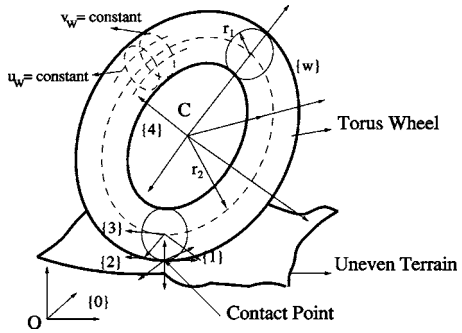

Fig. 1 Torus-shaped wheel on uneven terrain

$$\mathbf{\Phi}(t) + [\mathbf{\Psi}]\dot{\mathbf{q}} = \mathbf{0} \tag{4}$$

If there is no explicit dependence on time, t, as in our case, $\mathbf{\Phi}(t)$ is zero, and we can combine the holonomic and nonholonomic constraints to obtain the constraint equations as $[\mathbf{\Psi}]=\mathbf{0}$. For m holonomic and nonholonomic constraints, the constraint matrix is a $m\times n$ matrix and the constraint forces are given by $[\mathbf{\Psi}]^T\lambda$. The equations of motion can now be written as,

$$[\mathbf{M}(\mathbf{q})]\ddot{\mathbf{q}} + \mathbf{C}(\mathbf{q},\dot{\mathbf{q}})\dot{\mathbf{q}} + \mathbf{V}(\mathbf{q}) = \mathbf{Q} + [\mathbf{\Psi}]^T\lambda \tag{5}$$

where, $[\mathbf{M}(\mathbf{q})]$ is the $(n\times n)$ inertia matrix, $\mathbf{C}(\mathbf{q},\dot{\mathbf{q}})$ is the $(n\times n)$ matrix of centripetal and Coriolis acceleration terms, and $\mathbf{V}(\mathbf{q})$ is the $(n\times 1)$ vector containing gravity terms. Since $[\mathbf{M}(\mathbf{q})]$ is always invertible, Eq. (5) can be written as,

$$\ddot{\mathbf{q}} = [\mathbf{M}(\mathbf{q})]^{-1}(\mathbf{Q} - \mathbf{C}(\mathbf{q},\dot{\mathbf{q}})\dot{\mathbf{q}} - \mathbf{V}(\mathbf{q})) + [M(\mathbf{q})]^{-1}[\mathbf{\Psi}]^T\lambda \tag{6}$$

Differentiating the constraints $[\mathbf{\Psi}]\dot{\mathbf{q}}=\mathbf{0}$, we get

$$[\mathbf{\Psi}]\ddot{\mathbf{q}} + [\dot{\mathbf{\Psi}}]\dot{\mathbf{q}} = 0 \tag{7}$$

Substituting Eq. (6) in Eq. (7),

$$[\mathbf{\Psi}]\{[\mathbf{M}(\mathbf{q})]^{-1}(\mathbf{Q} - \mathbf{C}(\mathbf{q},\dot{\mathbf{q}})\dot{\mathbf{q}} - \mathbf{V}(\mathbf{q})) + [\mathbf{M}(\mathbf{q})]^{-1}[\mathbf{\Psi}]^T\lambda\} + [\dot{\mathbf{\Psi}}]\dot{\mathbf{q}} = 0 \tag{8}$$

Solving the Eq. (8) for λ we get,

$$\lambda = -\{[\mathbf{\Psi}][\mathbf{M}(\mathbf{q})]^{-1}[\mathbf{\Psi}]^T\}^{-1}\{[\dot{\mathbf{\Psi}}]\dot{\mathbf{q}} + [\mathbf{\Psi}][\mathbf{M}(\mathbf{q})]^{-1}(\mathbf{Q} - \mathbf{C}(\mathbf{q},\dot{\mathbf{q}})\dot{\mathbf{q}} - \mathbf{V}(\mathbf{q}))\} \tag{9}$$

After substituting Eq. (9) in Eq. (5), we get the equations of motion of a constrained dynamical system.

2.1 Equations of Motion for a Wheel. Figure 1 shows a torus wheel in single point contact with an uneven terrain. For the motion of the torus wheel on uneven terrain we choose the generalized coordinates $\mathbf{q}$ to be

$$\mathbf{q} = (u_w, v_w, u_g, v_g, \psi)^T \tag{10}$$

where, u_w, v_w are the coordinates of the point of contact on the wheel expressed in the frame $\{w\}$, u_g, v_g are the coordinates of the point of contact on the ground expressed in frame $\{0\}$ (see Fig. 1) and ψ is the angle between the X-axes of the two Gaussian frames at the point of contact. The transformation matrix of $\{w\}$ with respect to $\{0\}$ is given by

$${}^0_w[\mathrm{T}] = {}^0_1[\mathrm{T}]{}^1_2[\mathrm{T}]{}^2_3[\mathrm{T}]{}^3_4[\mathrm{T}]{}^4_w[\mathrm{T}]$$

$${}^0_w[\mathrm{T}] = \begin{pmatrix} {}^0_w[R] & {}^0\mathbf{p}_w \\ 0 & 1 \end{pmatrix} \tag{11}$$

where the individual transformation matrices are as given in Appendix A. In the above equation, ${}^0_w[R]$ represents the (3×3) rotational matrix which gives the orientation of the wheel in $\{0\}$ and $\mathbf{p_w}$ represents the position vector of the center of the wheel in $\{0\}$.

The kinematic equations of contact for the motion of the wheel on uneven terrain can be derived from Montana's contact equation [18] and is given as

$$(\dot{u}_w, \dot{v}_w)^T = [M_w]^{-1}([K_w] + [K^*])^{-1}[(-\omega_y, \omega_x)^T - [K^*](v_x, v_y)^T]$$

$$(\dot{u}_g, \dot{v}_g)^T = [M_g]^{-1}[R_\psi]([K_w] + [K^*])^{-1}[(-\omega_y, \omega_x)^T + [K_w](v_x, v_y)^T]$$

$$\dot{\psi} = \omega_z + [T_w][M_w](\dot{u}_w, \dot{v}_w)^T + [T_g][M_g](\dot{u}_g, \dot{v}_g)^T \tag{12}$$

$$0 = v_z$$

where $[M_{(\cdot)}]$, $[K_{(\cdot)}]$, $[T_{(\cdot)}]$ are the metric, curvature and torsion of the two surfaces (see [14,15] for details) and

$$[K^*] = [R_\psi][K_2][R_\psi]^T \tag{13}$$

with $[R_\psi]$ given by

$$[R_\psi] = \begin{pmatrix} \cos(\psi) & -\sin(\psi) \\ -\sin(\psi) & -\cos(\psi) \end{pmatrix}$$

In Eq. (12), ω_x, ω_y, and ω_z are the angular velocities and v_x, v_y, and v_z are the linear velocities of frame {2} relative to frame {1} expressed in frame {2}. To model *rolling without slip* v_x, v_y are set to zero in Eq. (12). It may be noted that $v_z=0$ ensures that the two surfaces do not loose contact.

The angular velocity of the wheel in {0} and the linear velocity of the wheel center in {0} can be obtained as

$$\hat{\Omega} = {}^0_w[\dot{R}]^0_w[R]^T = \begin{pmatrix} 0 & -\Omega_z & \Omega_y \\ \Omega_z & 0 & -\Omega_x \\ -\Omega_y & \Omega_x & 0 \end{pmatrix} \tag{14}$$

$${}^0\mathbf{V}_w = {}^0\dot{\mathbf{p}}_w \tag{15}$$

The angular velocity of the wheel ($\mathbf{\Omega} = (\Omega_x, \Omega_y, \Omega_z)^T$) and the linear velocity of its center ($\mathbf{V_w}$) can also be obtained from Eqs. (12) after appropriate frame transformations. The kinetic energy of the wheel is given by

$$\mathrm{KE} = \tfrac{1}{2}\mathbf{\Omega}^T[\mathbf{I}_w]\mathbf{\Omega} + \tfrac{1}{2}m_w{}^0\mathbf{V}_w{}^2 \tag{16}$$

where m_w is the mass of the wheel and $[\mathbf{I}_w]$ is the moment of inertia matrix of the wheel in $\{w\}$. In the case of the torus wheel $[\mathbf{I}_w]$ is given as

$$[\mathbf{I}_w] = \begin{pmatrix} \frac{1}{4}m_w(3r_1{}^2 + 4r_2{}^2) & 0 & 0 \\ 0 & \frac{1}{8}m_w(5r_1{}^2 + 4r_2{}^2) & 0 \\ 0 & 0 & \frac{1}{8}m_w(5r_1{}^2 + 4r_2{}^2) \end{pmatrix}$$

The potential energy of the wheel is given by

$$\mathrm{PE} = m_w g z_{wc} \tag{17}$$

where z_{wc} is the height of the center of the wheel in {0} and is obtained from the third component of the position vector of the center of the wheel, $\mathbf{p}_w$. The components of the mass matrix, M_{ij}, can be obtained by extracting from the kinetic energy term

$$\mathrm{KE} = \frac{1}{2}\sum_{i,j=1}^{5} M_{ij}\dot{q}_i\dot{q}_j$$

The components of the matrix of centrifugal and Coriolis terms, C_{ij}, can be obtained from the mass matrix as

$$C_{ij} = \frac{1}{2}\sum_{k=1}^{5}\left(\frac{\partial M_{ij}}{\partial q_k} + \frac{\partial M_{ik}}{\partial q_j} - \frac{\partial M_{kj}}{\partial q_i}\right)$$

The components of the vector of gravity terms $[\mathbf{V}(\mathbf{q})]$ can be obtained from the potential energy term as

$$V_i = \frac{\partial(\mathrm{PE})}{\partial q_i}$$

For motion without slip the nonholonomic constraints can be obtained from Eq. (12), and are given by

$$(v_x, v_y)^T = -[\mathbf{M}_w](\dot{u}_w, \dot{v}_w)^T + [\mathbf{R}_\psi][\mathbf{M}_g](\dot{u}_g, \dot{v}_g)^T = (0,0)^T \tag{18}$$

From the above, we can obtain the constraint matrix $[\mathbf{\Psi}]$ and hence its derivative $[\dot{\mathbf{\Psi}}]$. Using the matrices $[\mathbf{M}(\mathbf{q})]$, $[\mathbf{C}(\mathbf{q}, \dot{\mathbf{q}})]$, $[\mathbf{V}(\mathbf{q})]$, $[\mathbf{\Psi}]$, $[\dot{\mathbf{\Psi}}]$ and Eqs. (6) and (9) we form the equations of motion of a single wheel rolling without slip on uneven terrain. The algorithm for the solution of the dynamics problem is outlined below:

(1) *Generate the surface*:
The ground digital elevation model (DEM) is assumed to be known and a spline representation of the surface is generated. For dynamics, we need at least $\mathcal{C}^3$ continuity of the surface, ($\mathcal{C}^3$ continuity is required since $[\dot{\mathbf{\Psi}}]$ is required and $[\dot{\mathbf{\Psi}}]$ contains third partial derivatives of the surface function.) hence we can use a fourth degree B-spline to generate the surface. The surface representation and its derivatives are computed using built-in MATLAB functions.

(2) *Form the equations of motion*:
The equations of motion are formed in the manner outlined above. We have a set of 5 second order ODE's in 5 variables (namely, u_w, v_w, u_g, v_g, ψ) which can be solved with any ODE solver using appropriate initial conditions. The ODE's are formed symbolically using **Mathematica** [19].

(3) *Obtain initial conditions*:
The initial conditions are to be chosen such that they satisfy the nonholonomic constraints. The initial values for u_w, v_w, u_g, v_g, ψ can be chosen arbitrarily, depending on the desired position and orientation of the wheel in which we want to start. Among the first derivatives, namely $\dot{u}_w$, $\dot{v}_w$, $\dot{u}_g$, $\dot{v}_g$, $\dot{\psi}$, we can choose only three. The other two are to be determined from the nonholonomic no-slip constraints given by Eq. (18).

(4) *Solve equations of motion*:
The 5 second order equations of motion can be solved with appropriate ODE solver using initial conditions as obtained above. This gives the evolution of u_w, v_w, u_g, v_g, ψ and its first derivatives $\dot{u}_w$, $\dot{v}_w$, $\dot{u}_g$, $\dot{v}_g$, $\dot{\psi}$ in time.

2.2 Results and Discussion. We have tested the algorithm on various synthetically generated surfaces [15]. We present one such result for the motion of the torus wheel on the surface shown in the Fig. 2. In this simulation, we assume that there are no external applied force or moment acting on the wheel i.e., $\mathbf{Q_i}=0$. The initial conditions used are

$$u_g = 4.00103 \text{ m}, \quad v_g = 0.49346 \text{ m}, \quad u_w = 1.5698 \text{ rad},$$

$$v_w = 3\pi/2 \text{ rad}, \quad \psi = -3.141545 \text{ rad}, \quad \dot{u}_w = 0 \text{ rad/s},$$

$$\dot{v}_w = 2 \text{ rad/s}, \quad \dot{u}_g = 0 \text{ m/s}, \quad \dot{v}_g = 0.5975 \text{ m/s}, \quad \dot{\psi} = 0 \text{ rad/s}$$

.

Figure 3 shows the variation of wheel parameters, u_w, v_w, and ψ. It can be seen that the wheel tilts as it rolls on the uneven surface. Due to this, the trace of the wheel center and the contact point, as shown in Fig. 4, is different. Figure 5 shows that the wheel rolls without slip as the velocity components of the wheel contact point at the wheel-ground contact is almost 0. The conservation of energy is depicted by Fig. 6 which also shows the variation in potential and kinetic energy as the wheel moves over the uneven terrain.

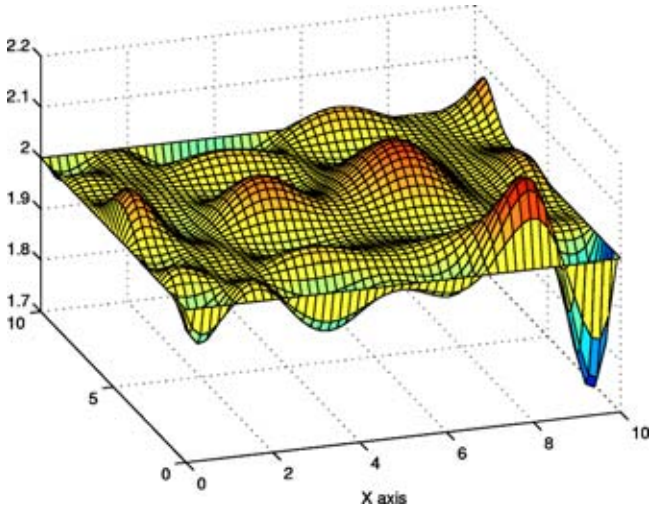

Fig. 2 Uneven terrain used for simulations

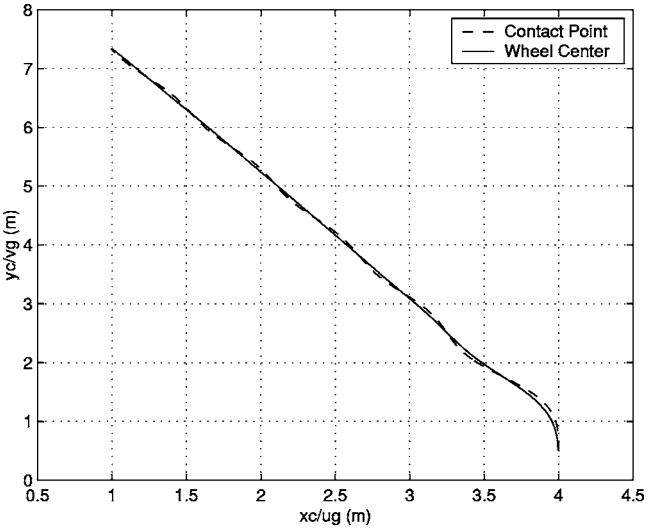

Fig. 4 Locus of wheel center and ground contact point for single wheel moving on uneven terrain

3 Kinematics of the Three-wheeled WMR

For motion of a WMR on uneven terrain without slip we propose a model of a three-wheeled mobile robot consisting of three toroidal wheels attached to a rigid (moving) platform by rotary joints. The rear wheels have two rotary joints with one of the joints being passive and one actuated. The passive joint allows lateral rotation of the toroidal wheels (i.e., rotation about an axis perpendicular to the axle and lying in the plane of the platform) and the actuated joint represents a motor or an actuator for in-plane rotation of the wheel. The front wheel can be steered (i.e., rotated about an axis perpendicular to the plane of the top platform) and it has no lateral tilt capability. In this configuration, we can model the vehicle instantaneously as an equivalent hybrid series-parallel mechanism as shown in Fig. 7. As mentioned in Eq. (12), at the wheel-ground contact point, we have one holonomic constraint, $v_z=0$, which ensures contact is always maintained. Moreover, at each instant, we have 2 nonholonomic constraints which prevents instantaneous sliding, and these are $v_x=0$ and $v_y=0$. Intuitively, this suggests us to model the wheel-ground contact point, *instantaneously* as a three-degree-of-freedom (DOF) joint. It may be noted that this joint is different from a three-DOF spherical joint due to the presence of 2 nonholonomic constraints which restrict the motion at any instant *only* in terms of achievable velocities and we call this a "nonholonomic" joint. The other joints in the mechanism, namely the joints allowing rotation of the wheel, lateral tilt, and steering, are modeled as traditional 1 DOF rotary joints.

Now using Gruebler's criterion for a mechanism

$$\mathrm{DOF} = 6(n - j - 1) + \sum f_i \tag{19}$$

we find the DOF of the mechanism as 3, with total number of links n as 8, number of joints j as 9, and the total number of degrees of freedom (3 for each wheel ground contact and 1 for each of the 6 rotary joints), $\Sigma f_i=15$. Therefore, three of the joint variables should be actuated and we choose rotation at the two rear wheels, θ_1 and θ_2, and the steering at the front wheel, ϕ_3, as the actuated variables. The two lateral tilts at the rear wheels, δ_1 and δ_2, and the rotation of the front wheel θ_3 are the passive variables which need to be computed. As the vehicle is subjected to nonholonomic (and nonintegrable) no-slip constraints, the inverse kinematics problem can at best be formulated in terms of the

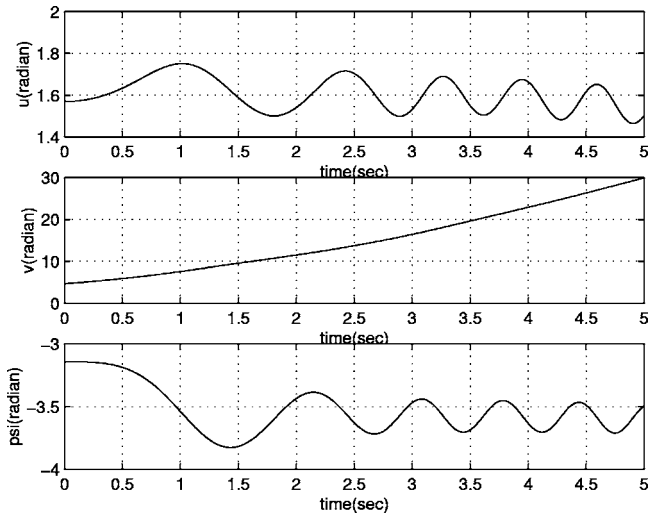

Fig. 3 Variation of parameters for single wheel moving on uneven terrain

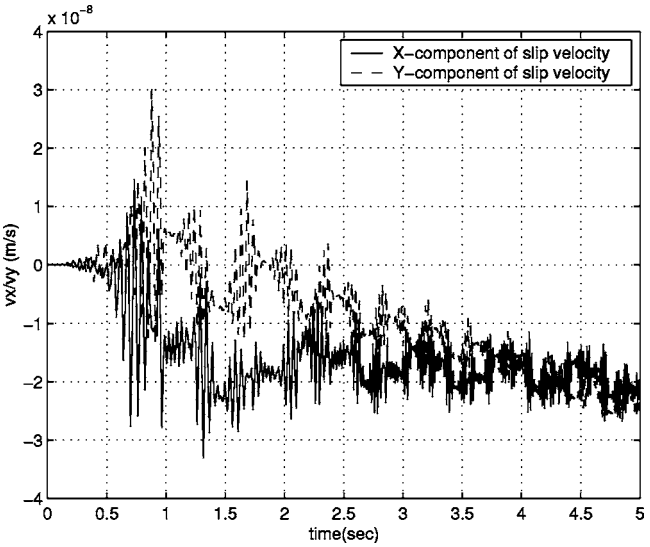

Fig. 5 Components of slip velocity at the wheel ground contact point

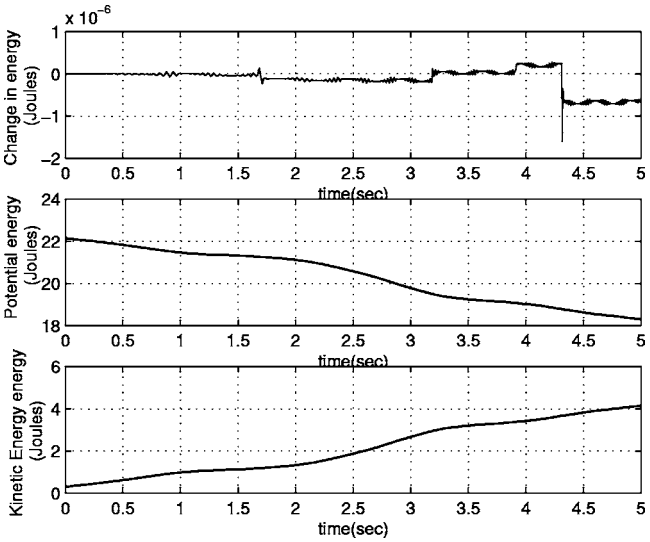

Fig. 6 Conversation of energy and the variation of potential and kinetic energy

first derivatives of the kinematic variables and the kinematic variables are obtained by integration. The inverse kinematics problem for the 3-DOF vehicle can be stated as:

Given any three of the velocities of the top platform V_{p_x}, V_{p_y}, V_{p_z}, Ω_{p_x}, Ω_{p_y}, Ω_{p_z} (V_{p_x}, V_{p_y}, V_{p_z} are the components of the linear velocity vector of the center of the platform or any other point of interest and Ω_{p_x}, Ω_{p_y}, Ω_{p_z} are the components of the angular velocity vector of the platform) and the geometric properties of the ground and wheel, find the two drive inputs to the rear wheels ($\dot{\theta}_1$, $\dot{\theta}_2$) and the steering input to the front wheel ($\dot{\phi}_3$) (Instead of the angular velocities Ω_{p_x}, Ω_{p_y}, Ω_{p_z}, we may use the Euler angle rates $\dot{\alpha}$, $\dot{\beta}$, $\dot{\gamma}$, where γ, β, α is a 3-2-1 Euler angle parametrization of orientation.)

To solve this problem we proceed as follows:

(1) *Generate the Surface*:
As described in Sec. 2, we use B-splines to reconstruct the surface from elevation data. From the interpolated surface we find expressions for the metric, curvature and torsion form for the ground. We also obtain expressions for the metric, curvature and torsion form for the torus shaped wheel.

(2) *Form contact equations*:
For each wheel we write the 5 differential equations [see Eq. (12)], yielding a total of 15 ODE's in 15 contact variables u_{w_i}, v_{w_i}, u_{g_i}, v_{g_i}, and ψ_i, where $i=1,2,3$. Since the wheels undergo no-slip motion, we set $v_x=v_y=0$ for each of the wheels in Eq. (12).

3 *Relate angular velocities of wheel and platform*:

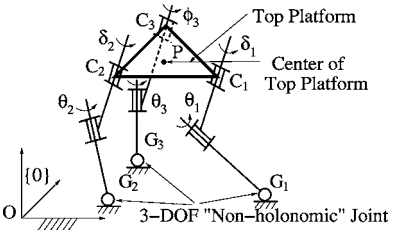

Fig. 7 Equivalent instantaneous mechanism for the 3-DOF WMR

The quantities ω_x, ω_y, and ω_z in the contact equations for each wheel are the three components of angular velocities of frame {2} with respect to frame {1} and are unknown. These are related to the angular velocity of the platform Ω_x, Ω_y, Ω_z and the input and passive joint rates. In the fixed coordinate system, {0}, we can write for each wheel

$$^0(\omega_x,\omega_y,\omega_z)^T = {}^0(\Omega_{p_x},\Omega_{p_y},\Omega_{p_z})^T + {}^0\omega_{\text{input}} \tag{20}$$

where the skew symmetric form of $^0\omega_{\text{input}}$ can be written for each wheel as

$$^0\hat{\omega}_{\text{input}} = {}^0[\dot{\mathbf{R}}]_{\text{in}}\,{}^0[\mathbf{R}]_{\text{in}}{}^T$$

$$^0[\mathbf{R}]_{\text{in}} = {}^0_p[\mathbf{R}][\mathbf{R}(\mathbf{e}_3,\phi_i)][\mathbf{R}(\mathbf{e}_2,\delta_i)][\mathbf{R}(\mathbf{e}_1,\theta_i)] \quad i=1,\ 2 \text{ or } 3$$

and $\mathbf{e}_1=(1,0,0)^T$, $\mathbf{e}_2=(0,1,0)^T$, $\mathbf{e}_3=(0,0,1)^T$. Note that for the 3-DOF vehicle $\phi_1=\phi_2=\delta_3=0$.

The above Eq. (20) couples all 5 sets of ODE's and we get a set of 15 coupled ODE's in 21 variables. These are the 15 contact variables u_{w_i}, v_{w_i}, u_{g_i}, v_{g_i}, ψ_i ($i=1,2,3$), the 3 wheel rotations θ_1, θ_2, θ_3, the 2 lateral tilts δ_1, δ_2, and the front wheel steering ϕ_3. Out of these, the rates of the three actuated variables, θ_1, θ_2, and ϕ_3, are assumed to be known.

(4) *Obtain velocity of platform*:
The angular velocity and the linear velocity of the center of the platform can be expressed in terms of the 15 wheel variables u_i, v_i, u_{g_i}, v_{g_i}, ψ_i ($i=1,2,3$) and its first derivatives with respect to time. If γ, β, α be a 3-2-1 Euler angle parametrization representing the orientation of the platform we hav

$$\begin{aligned}
^0\Omega_{p_x} &= \dot{\alpha}\cos(\beta)\cos(\gamma) - \dot{\beta}\sin(\gamma)\\
&= f_1(u_i,v_i,u_{g_i},v_{g_i},\psi_i,\dot{u}_i,\dot{v}_i,\dot{u}_{g_i},\dot{v}_{g_i},\dot{\psi}_i)\\
^0\Omega_{p_y} &= \dot{\alpha}\cos(\beta)\sin(\gamma) + \dot{\beta}\cos(\gamma)\\
&= f_2(u_i,v_i,u_{g_i},v_{g_i},\psi_i,\dot{u}_i,\dot{v}_i,\dot{u}_{g_i},\dot{v}_{g_i},\dot{\psi}_i)\\
^0\Omega_{p_z} &= \dot{\gamma} - \dot{\alpha}\sin(\beta)\\
&= f_3(u_i,v_i,u_{g_i},v_{g_i},\psi_i,\dot{u}_i,\dot{v}_i,\dot{u}_{g_i},\dot{v}_{g_i},\dot{\psi}_i) \quad i=1,2,3
\end{aligned} \tag{21}$$

Also, let x_c, y_c, z_c be the coordinates of the center of the platform in {0}. The linear velocity of the center of the platform is given by

$$^0(V_{p_x},V_{p_y},V_{p_z})^T = {}^0(\dot{x}_c,\dot{y}_c,\dot{z}_c)^T = {}^0\mathbf{V}_{w_i} + {}^0(\Omega_{p_x},\Omega_{p_y},\Omega_{p_z})^T \times {}^0P_{c_i} \tag{22}$$

where i stands for any one of the 3 wheels 1, 2 or 3, $^0P_{c_i}$ is the point of attachment of the wheel to the platform from the center of the platform expressed in frame {0}, $\mathbf{V}_{w_i}$ is the velocity of the center of the wheel.

(5) *Form holonomic constraint equations*:
In addition to the contact equations, for the 3 wheels to form a vehicle they must satisfy 3 holonomic constraint equations (refer to Fig. 7), namely

$$(\mathbf{OC}_1-\mathbf{OC}_2)^2 = \mathbf{l_{12}}^2; \quad (\mathbf{OC}_1-\mathbf{OC}_3)^2 = \mathbf{l_{13}}^2; \tag{23}$$

$$(\mathbf{OC}_3-\mathbf{OC}_2)^2 = \mathbf{l_{32}}^2;$$

where $\mathbf{OC}_1$, $\mathbf{OC}_2$, $\mathbf{OC}_3$ are the position vectors of the center of the three wheels, C_1, C_2, C_3, respectively from the origin $\mathbf{O}$ of the fixed frame and l_{ij} is the distance between center of wheels i and j, respectively.

The above steps leads to a system of 24 equations in 27 variables which can be written as

$$[\mathbf{\Psi}]\dot{\mathbf{q}} = 0 \tag{24}$$

where $\mathbf{\Psi}$ is a 24×27 matrix. The 27 variables (generalized coordinates) are as follows: 15 contact variables u_i, v_i, u_{g_i}, v_{g_i}, ψ_i, $i = \mathbf{1},\mathbf{2},\mathbf{3}$; **3** passive variables δ_1, δ_2, θ_3; 3 actuated variables θ_1, θ_2, ϕ_3; and 6 variables, α, β, γ, x_c, y_c, z_c denoting the orientation of the platform and the position of its center. These system of equations can be obtained symbolically using **Mathematica** and can then solved with appropriate initial conditions (the reader is referred to [15] for simulation results and details). In the next section, we formulate the dynamic equations of motion, in terms of the 27 generalized coordinates, as a set of 27 ordinary differential equations subjected to the 24 constraints given in Eq. (24).

4 Dynamic Analysis of the Three-wheeled WMR

To obtain the dynamic equations of motion a Lagrangian formulation was used. We considered the use of a commercially available dynamics simulation software such as ADAMS. However, we faced several difficulties for this particular problem. Firstly, we want no-slip nonholonomic constraint be satisfied between the uneven ground and the wheel, and secondly we want contact between a torus and an arbitrary uneven surface. Although it is possible to ensure point-curve and curve-curve contact in Adams [20], to ensure point contact between two arbitrary surfaces and 3D relative motion between the two surfaces can only be done by very complicated models using several joints and links. In addition, to the best of our knowledge, it is not very easy to impose nonholonomic constraints between two arbitrary surfaces in point contact. The ADAMS CAR module assumes a certain tire profile which is used to obtain a contact patch and subsequent contact force calculations. Our model on the other hand assumes single point contact and our endeavor is to demonstrate no-slip motion for our WMR design. Therefore, we decided to derive the equations of motion using the symbolic algebra package **Mathematica**, and this is described in this section.

4.1 Formulation of the Equations of Motion. Let KE and PE denote the total kinetic energy and the total potential energy of the vehicle respectively. The KE (PE) of the vehicle is the sum of the kinetic energy (potential energy) of the 3 wheels, the platform, the actuators and the links and can be written as given below:

$$\begin{aligned}\mathrm{KE} &= (\mathrm{KE})_{w_1} + (\mathrm{KE})_{w_2} + (\mathrm{KE})_{w_3} + (\mathrm{KE})_{\text{platform}} + (\mathrm{KE})_{\text{actuators}} \\ &\quad + (\mathrm{KE})_{\text{links}} \end{aligned} \tag{25}$$

$$\begin{aligned}\mathrm{PE} &= (\mathrm{PE})_{w_1} + (\mathrm{PE})_{w_2} + (\mathrm{PE})_{w_3} + (\mathrm{PE})_{\text{platform}} + (\mathrm{PE})_{\text{actuators}} \\ &\quad + (\mathrm{PE})_{\text{links}}\end{aligned}$$

where w_i, $i=1,2,3$ are the three wheels, $(.)_{\text{actuators}}$ denote the contribution of motor inertia at the two rear wheels and the front steering wheel, and $(.)_{\text{links}}$ denote the contribution from the passive links. The kinetic energy and potential energy of each wheel can be obtained as outlined in the previous section. The kinetic energy of each wheel is given by

$$\mathrm{KE} = \tfrac{1}{2}\mathbf{\Omega}^T[\mathbf{I}_w]\mathbf{\Omega} + \tfrac{1}{2}m_w^0\mathbf{V}_w^2$$

where m_w is the mass of the wheel and $[\mathbf{I}_w]$ is the moment of inertia matrix of the wheel in $\{w\}$ (refer to Fig. 1), $\mathbf{\Omega}$ is the angular velocity of the wheel, $\mathbf{V}_w$ is the linear velocity of the center of the wheel. The potential energy of each wheel is given by

$$\mathrm{PE} = m_w g z_{wc} \tag{26}$$

where z_{wc} is the height of the center of the wheel in $\{0\}$ which is given by the third component of the position vector of the center of the wheel, $\mathbf{p}_w$.

The kinetic energy of the platform is given by

$$(\mathrm{KE})_{\text{platform}} = \tfrac{1}{2}m_p(\dot{x}_c^2 + \dot{y}_c^2 + \dot{z}_c^2) + \tfrac{1}{2}\Omega_p^T[I_p]\Omega_p \tag{27}$$

where $\Omega_p = \left[{}^p_0R\right]^T\left[{}^p_0\dot{R}\right]$ is the angular velocity of the platform in its body frame $\{p\}$, m_p is the mass of the platform, $[I_p]$ is the mass moment of inertia of the platform in its body frame, and $(x_c, y_c, z_c)^T$ is the position vector of the center of the platform in the fixed frame $\{0\}$. The potential energy of the platform is given by

$$(\mathrm{PE})_{\text{platform}} = m_p g z_c \tag{28}$$

The mass of the passive joints allowing lateral tilt is assumed to be lumped with the mass of the platform and that of the actuators is assumed to be lumped with the wheel. Thus, the contribution to the potential energy term and the kinetic energy term (due to linear velocity) is included in the kinetic energies of wheel and platform. As shown in the equivalent mechanism model in Fig. 7, the passive joint assembly and the actuators for each wheel form a serial chain from the ground to the platform body (G_iC_i, $i=1,2,3$). Along the same lines as the analysis in serial manipulators, we can obtain the rotational kinetic energy of the passive joint assemblies and actuators. For the two rear wheels, the angular velocity of the passive joint assembly in a local coordinate system fixed to the joint is

$$\mathbf{\Omega}_{\text{links}_i} = [\mathbf{R}(e_2, \delta_i)]^{Tp}\mathbf{\Omega}_p + (0, \dot{\delta}_i, 0)^T \quad \text{for} \quad i = 1,2$$

where e_1, e_2, e_3 (Note that in this discussion we have used the same symbols e_1, e_2, e_3, for representing the unit vectors at the coordinate frames fixed to each of the joints. This is just for notational simplicity, and e_1, e_2, e_3, are not the same for all the joints.) are the unit vectors of the local coordinate frame attached to the passive joint, with e_2 being the local axis of rotation and ${}^p\Omega_p$ is the angular velocity of the platform in the frame attached to the center of the platform. The rotational kinetic energy of the passive links for the two rear wheels (wheel 1 and 2) can then be easily obtained by

$$\mathrm{KE}_{\text{links}_i} = \tfrac{1}{2}\mathbf{\Omega}^T_{\text{links}_i}[\mathbf{I}_{\text{links}_i}]\mathbf{\Omega}_{\text{links}_i} \quad \text{for} \quad i = 1,2$$

where $[\mathbf{I}_{\text{links}_i}]$, $i=1,2$, is the mass moment of inertia of the passive links. The angular velocity of the two actuators are given in a local frame fixed to the actuated joints (whose unit vectors are e_1, e_2, e_3 with e_1 being the local axis of rotation) by

$$\mathbf{\Omega}_{\text{actuators}_i} = [\mathbf{R}(e_1, \theta_i)]^T\mathbf{\Omega}_{\text{links}_i} + (\dot{\theta}_i, 0, 0)^T \quad \text{for} \quad i = 1,2$$

The rotational kinetic energy of the actuators are thus given by

$$\mathrm{KE}_{\text{actuators}_i} = \tfrac{1}{2}\mathbf{\Omega}^T_{\text{actuators}_i}[\mathbf{I}_{\text{actuators}_i}]\mathbf{\Omega}_{\text{actuators}_i} \quad \text{for} \quad i = 1,2$$

where $[\mathbf{I}_{\text{actuators}_i}]$, $i=1,2$, is the mass moment of inertia of the actuators. The angular velocity of the actuator (in a local frame fixed to the actuated joint whose unit vectors are e_1, e_2, e_3 with e_3 being the local axis of rotation) steering the front wheel is given by

$$\mathbf{\Omega}_{\text{actuators}_i} = [\mathbf{R}(e_3, \phi_i)]^{Tp}\mathbf{\Omega}_p + (0, 0, \dot{\phi}_i)^T \quad \text{for} \quad i = 3$$

Therefore, the rotational kinetic energy of the steering actuator is given by

$$\mathrm{KE}_{\text{actuators}_i} = \tfrac{1}{2}\mathbf{\Omega}^T_{\text{actuators}_i}[\mathbf{I}_{\text{actuators}_i}]\mathbf{\Omega}_{\text{actuators}_i} \quad \text{for} \quad i = 3$$

The angular velocity of the passive joint and link in the front wheel (wheel 3) allowing in-plane rotation of the wheel in a frame fixed to the unactuated joint (whose unit vectors are e_1, e_2, e_3 with e_1 being the local axis of rotation) is given by

$$\mathbf{\Omega}_{\text{links}_i} = [\mathbf{R}(e_1, \theta_i)]^T\mathbf{\Omega}_{\text{actuators}_i} + (\dot{\theta}_i, 0, 0)^T \quad \text{for} \quad i = 3$$

The rotational kinetic energy is given by

$$\mathrm{KE}_{\mathrm{links}_i} = \tfrac{1}{2}\boldsymbol{\Omega}^T_{\mathrm{links}_i}[\mathbf{I}_{\mathrm{links}_i}]\boldsymbol{\Omega}_{\mathrm{links}_i} \quad \text{for} \quad i=3$$

The above steps gives us the total kinetic energy of the passive joint assemblies and the actuators.

Once we have the total kinetic energy, the components of the mass matrix can be obtained from

$$\mathrm{KE} = \frac{1}{2}\sum_{i,j=1}^{27} M_{ij}\dot{q}_i\dot{q}_j$$

The components of the matrix of centrifugal and Coriolis terms, C_{ij}, can be obtained from the mass matrix by

$$C_{ij} = \frac{1}{2}\sum_{k=1}^{27}\left(\frac{\partial M_{ij}}{\partial q_k} + \frac{\partial M_{ik}}{\partial q_j} - \frac{\partial M_{kj}}{\partial q_i}\right)$$

The components of the vector of gravity terms $[V(\mathbf{q})]$ can be obtained from the potential energy term and is given by

$$V_i = \frac{\partial(\mathrm{PE})}{\partial q_i}$$

The three-wheeled WMR for no-slip motion is subjected to both nonholonomic and holonomic constraints. The nonholonomic constraints arise out of the no-slip conditions at the wheel ground contact points. The holonomic constraints arise out of the fact that the three wheels are attached to a rigid platform and also that the coordinates of the position and orientation of the platform can be expressed in terms of the other variables. The constraint equations are 24 in number and are the same as the set of inverse kinematics equations (27).

The equations of motion were generated by extensive symbolic computation using the software package **Mathematica** [9]. They can be expressed in the form

$$[\mathbf{M}(\mathbf{q})]\ddot{\mathbf{q}} + \mathbf{C}(\mathbf{q},\dot{\mathbf{q}})\dot{\mathbf{q}} + \mathbf{V}(\mathbf{q}) = \tau + [\boldsymbol{\Psi}]^{\mathbf{T}}\lambda \tag{29}$$

where $[\mathbf{M}(\mathbf{q})]$ is a 27×27 symmetric positive definite mass matrix, $\mathbf{C}(\mathbf{q},\dot{\mathbf{q}})\dot{\mathbf{q}}$, $\mathbf{V}(\mathbf{q})$ are 27×1 vectors representing the Coriolis/centrifugal terms and gravity terms, respectively, and τ is a 27×1 vector of external forces/torques. It may be noted that only 3 elements of τ corresponding to the actuated variables θ_1, θ_2, ϕ_3 are nonzero and all others are zero. The 24×1 vector of the Lagrange multipliers λ can be obtained from the 24 constraint equations as outlined in Sec. 2.

On solving the equations of motion on a flat plane with the actuators locked and the rear wheels tilted, we observed that the wheels fell under the action of gravity. This is apparently contrary to the fact that any parallel manipulator (or hybrid series-parallel manipulator) with its actuators locked, behave as a structure under any external loading (for example, at a nonsingular configuration, a Stewart platform with all its actuators locked can resist any external forces and moments). It is to be noted that in our equivalent mechanism model the 3-DOF joints at the wheel ground contact points are not spherical joints. They are 3-DOF nonholonomic joints which arise from no-slip constraints and they allow motion as long as the no-slip constraints are not violated, i.e., they only restrict the space of achievable velocities and *not* the space of position and orientation variables. This is the reason for which the wheels fall under gravity. To prevent falling of the wheels, we propose the use of a flexible coupling between the actuator and the platform body (similar to a suspension) which limits the lateral tilt of the wheels. For our modeling purposes, we have assumed the system to be a simple spring-mass-damper system. (The ADAMS CAR module has several advanced features of modeling suspensions and other vehicle components, and we will attempt to use these features for detail design of a prototype WMR planned for future.) The spring and damping force has been added to the right-hand side of the equations of motion. Hence, in the vector τ, there are two additional terms of the form $k_i\delta_i + c_i\dot{\delta}_i$, $i=1,2$ (k_i is the stiffness of the flexible coupling and c_i is the damping), in the equations corresponding to δ_1 and δ_2. In our simulation, we have estimated the numerical values of k_i and c_i, $i=1,2$ as outlined in Sec. 5.

4.2 Algorithm for Solving the Dynamic Equations of Motion. The key steps in solving the dynamics of the three-wheeled WMR are summarized below:

(1) *Generate the surface*:
As before, we assume the terrain DEM to be known and we generate a spline representation of the surface. For dynamics, we need $\mathcal{C}^3$ continuity of the surface, hence we use a fourth degree B-spline to generate the surface. The surface representation and its derivatives are computed using inbuilt MATLAB [21] functions.

(2) *Form equations of motion*:
The equations of motion are formed in the manner outlined above. We have a set of 27 second order ODE's in 27 variables which can be solved with any ODE solver using appropriate initial conditions. The ODE's are formed symbolically using **Mathematica** [9].

(3) *Obtain initial conditions*:
The initial conditions for the configuration variables are determined in the same manner as those for the inverse kinematics problem. For the first derivatives of these variables, the initial conditions are to be chosen such that they satisfy the no-slip nonholonomic constraints at the initial instant. We choose 3 of them arbitrarily and determine the other 24 by solving the 24 constraint equations which are linear in the first derivatives of the configuration variables. Essentially, this involves the solution of 24 linearly independent linear equations for 24 variables.

(4) *Solve equations of motion*:
The 27 second order equations of motion are solved with a ODE solver using initial conditions as obtained above. This gives the evolution of u_i, v_i, u_{g_i}, v_{g_i}, ψ_i, $i=1,2,3$ and its first derivatives $\dot{u}_i$, $\dot{v}_i$, $\dot{u}_{g_i}$, $\dot{v}_{g_i}$, $\dot{\psi}_i$ in time. We also obtain the variation of the passive lateral tilts and their rates, the actuator rates and the position of the center of the platform and its orientation as a function of time. It may be mentioned that such a large set of DAE's usually needs sophisticated stiff solvers. However, in our numerical simulations, the ODE45 routine in MATLAB [21] was observed to be adequate.

5 Results and Discussion

We have tested our dynamics formulation on a variety of B-spline surfaces (for details, see [15]). In this section, we present a simulation result of the vehicle moving on the surface shown in Fig. 2. The mass and inertia of the various components used in our simulations are as given below:

Mass of the platform (and passive joint assemblies)$=m_p=10$ kg.

Mass of each wheel (and actuators)$=m_w=1$ kg.

Mass Moment of inertia of each actuator (in SI units)

$$[\mathbf{I}_{\mathrm{actuators}_i}] = \begin{pmatrix} 0.1 & 0 & 0 \\ 0 & 0.1 & 0 \\ 0 & 0 & 0.1 \end{pmatrix} \quad \text{for} \quad i=1,2,3$$

Mass Moment of inertia of passive joint assembly (in SI units)

$$[\mathbf{I}_{\mathrm{links}_i}] = \begin{pmatrix} 0.1 & 0 & 0 \\ 0 & 0.1 & 0 \\ 0 & 0 & 0.1 \end{pmatrix} \quad \text{for} \quad i=1,2,3$$

The stiffness (k_i) of the flexible coupling is obtained by modeling it as a simple linear torsional spring. We have assumed that

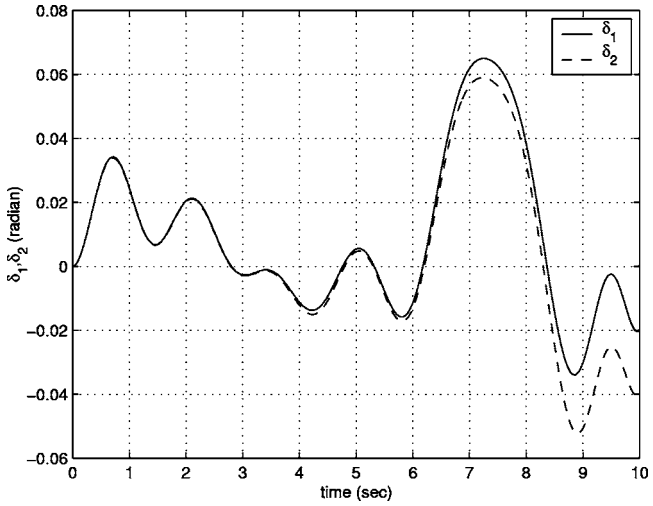

Fig. 8 Variation of δ_1, δ_2

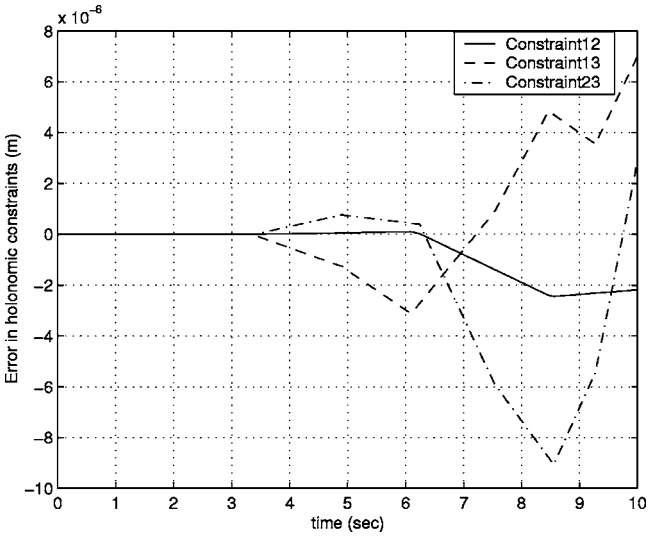

Fig. 9 Constraint satisfaction for the 3-wheeled WMR moving on uneven terrain

the spring has a maximum allowable deflection of $\delta_{\max}=\pi/4$, under static loading, with a load of $W/3(r_1+r_2)$ N m, where, $W=(m_p+3m_w)g$ N, is the total weight of the vehicle. The damping coefficient (c_i) is assumed to be 5% of the stiffness. Although, the procedure of choosing the values of stiffness and damping is quite elementary, it serves the main purpose of demonstrating the fact that the wheels of the three-wheeled WMR do not fall due to self-weight and the WMR can negotiate uneven terrain without slip. The actual values of k_i and c_i would depend upon the detailed design of the flexible joint assembly and this issue is not addressed here. The numerical values of k_i and c_i used in our simulation are $k_i=16.2376$ N m/rad and $c_i=0.574$ N ms/rad.

The initial conditions used for the simulation are: $u_1=1.57$ rad, $v_1=3\pi/2$ rad, $u_{g_1}=5.008$ m, $v_{g_1}=1.5067$ m, $\psi_1=-3.142$ rad, $u_2=1.5648$ rad, $v_2=3\pi/2$ rad, $u_{g_2}=4$ m, $v_{g_2}=1.5$ m, $\psi_2=-3.1418$ rad, $u_3=1.5818$ rad, $v_3=3\pi/2$ rad, $u_{g_3}=4.4897$ m, $v_{g_3}=2.483$ m, $\psi_3=-3.1419$ rad, $\theta_1=0$ rad, $\theta_2=0$ rad, $\theta_3=0$ rad, $\delta_1=0$ rad, $\delta_2=0$ rad, $\phi_3=0$ rad, $z_c=2.3088$ m, $\alpha=-0.0127$ rad, $\beta=0.0133$ rad. All the initial values of the first derivatives are assumed to be 0. The procedure to obtain these consistent initial conditions are described in [15].

The inputs used are the two driving actuator torques and one steering torque are $\tau_1=-0.35$ N m, $\tau_2=-0.5$ N m, and $\tau_3=-0.001t$ N m.

The variation of lateral tilts of the rear wheels is shown in Fig. 8. The satisfaction of holonomic constraints is depicted in Fig. 9, and the locus of the wheel center's, wheel-ground contact points and the center of the platform is shown in Fig. 10. Figure 11 shows that there is no-slip at the wheel ground contact points of the three wheels.

6 Conclusion

In this paper, we have obtained and solved the equations of motion for a proposed three-wheeled WMR designed for motion without slip on uneven terrain. We have used a Lagrangian approach for deriving the equations of motion and provided simulation results showing that the proposed vehicle can negotiate uneven terrain without slip. We are currently in the process of building a prototype along the lines of our proposed architecture and future work involves field testing of the prototype.

Appendix A

The transformation matrices for going from frame {0} to frame {*w*} are as follows:

$$ {}^{0}_{1}[\mathbf{T}] = \begin{pmatrix} l_1 & m_1 & n_1 & u_g \\ l_2 & m_2 & n_2 & v_g \\ l_3 & m_3 & n_3 & f(u_g,v_g) \\ 0 & 0 & 0 & 1 \end{pmatrix} $$

where l_i, m_i, n_i, $i=1,2,3$ are the components of the orthogonal vectors $\{\mathbf{f}_u/|\mathbf{f}_u|, \mathbf{f}_v/|\mathbf{f}_v|, \mathbf{n}\}$, $\mathbf{n}$ as defined in Sec. 2.

$$ {}^{1}_{2}[\mathbf{T}] = \begin{pmatrix} \cos\psi & -\sin\psi & 0 & 0 \\ -\sin\psi & -\cos\psi & 0 & 0 \\ 0 & 0 & -1 & 0 \\ 0 & 0 & 0 & 1 \end{pmatrix} $$

$$ {}^{2}_{3}[\mathbf{T}] = \begin{pmatrix} \sin u & 0 & \cos u & 0 \\ 0 & 1 & 0 & 0 \\ -\cos u & 0 & \sin u & -r_1 \\ 0 & 0 & 0 & 1 \end{pmatrix} $$

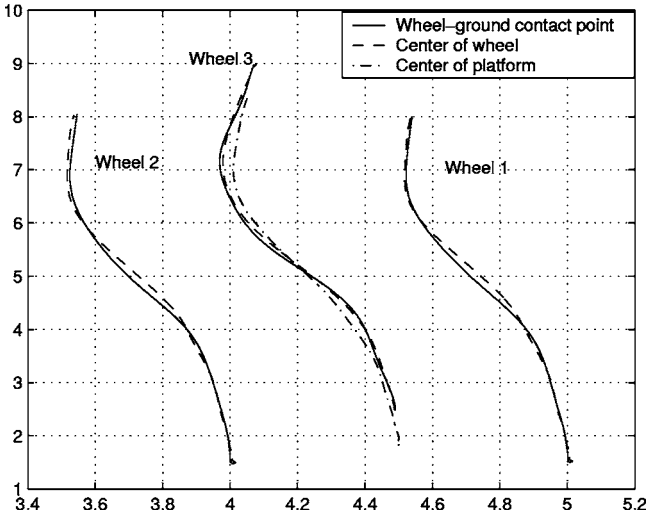

Fig. 10 Locus of wheel-ground contact point, wheel center and platform center of the 3-wheeled WMR on uneven terrain

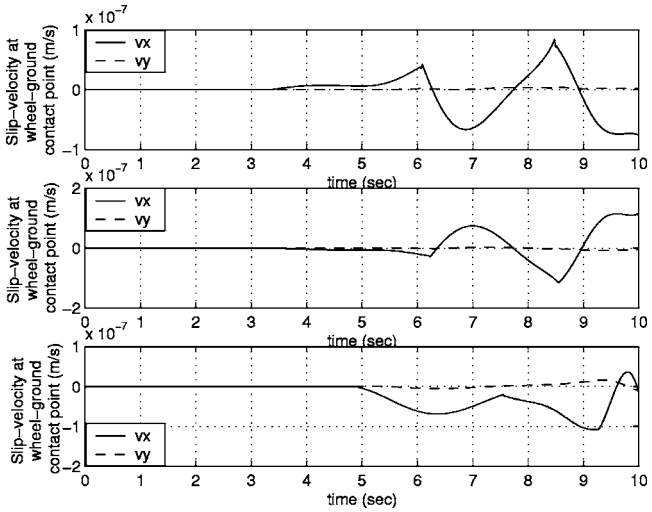

Fig. 11 Verification of no-slip constraints at wheel-ground contact point

$$
{}^{3}_{4}[\mathbf{T}] = \begin{pmatrix} 1 & 0 & 0 & 0 \\ 0 & -\sin v & \cos v & 0 \\ 0 & -\cos v & -\sin v & -r_2 \\ 0 & 0 & 0 & 1 \end{pmatrix}
$$

$$
{}^{4}_{w}[\mathbf{T}] = \begin{pmatrix} -1 & 0 & 0 & 0 \\ 0 & 1 & 0 & 0 \\ 0 & 0 & -1 & 0 \\ 0 & 0 & 0 & 1 \end{pmatrix}
$$

References

[1] Waldron, K. J., 1995, "Terrain Adaptive Vehicles," J. Mech. Des., **117B**, pp. 107–112.

[2] Alexander, J. C., Maddocks, J. H., 1989, "On the kinematics of wheeled mobile robots," Int. J. Robot. Res., **8**, pp. 15–27.

[3] Muir, P. F., and Neuman, C. P., 1987, "Kinematic modeling of wheeled mobile robots," J. Rob. Syst., **4**, pp. 281–329.

[4] Bickler, D. B., 1998, "Roving over Mars," Mech. Eng. (Am. Soc. Mech. Eng.), **120**, pp. 74–77.

[5] Sreenivasan, S. V., and Waldron, K. J., 1996, "Displacement analysis of an actively articulated wheeled vehicle configuration with extension to motion planning on uneven terrain," J. Mech. Des., **118**, pp. 312–317.

[6] Wilcox, B. H., and Gennery, D. B., 1987, "A Mars rover for the 1990's," J. Br. Interplanet. Soc., **40**, pp. 484–488.

[7] Choi, B. J., Sreenivasan, S. V., and Davis, P. W., 1999, "Two wheels connected by an unactuated variable length axle on uneven ground: Kinematic modeling and experiments," ASME J. Mech. Des., **121**, pp. 235–240.

[8] Davis, P. W., Sreenivasan, S. V., and Choi, B. J., 1997, "Kinematics of two wheels joined by a variable-length axle on uneven terrain," Proceedings of the ASME DETC'97, Paper No. DETC97/DAC-3857.

[9] Sreenivasan, S. V., and Nanua, P., 1996, "Kinematic Geometry of Wheeled Vehicle systems," 24th ASME Mechanisms Conference, Irvine, CA, 96-DETC-MECH-1137.

[10] Choi, B. J., and Sreenivasan, S. V., 1999 "Gross motion characteristics of articulated robots with pure rolling capability on smooth uneven surfaces," IEEE Trans. Rob. Autom., **15**, pp. 340–343.

[11] Mackle, G., Schirle, T., 2002, "Active Tire Tilt Control—Das Neue Fahrwerkkonzept Des F400 Carving," "11th Aachen colloquium on Vehicle and Engine Technology, RWTH," Vol. 1.

[12] Harty, D., 2003, "Brand-by-Wire—A Possiblity" SAE International Congress and Exhibition, Paper No 2003-01-0097, Detroit, MI, March 2003.

[13] Zachrison, A., Rösth, M., Andersson, J., and Werndin, R., 2003, "EVOLVE a vehicle based test platform for active rear axle camber and steering control," SAE International Congress and Exhibition, Paper No. 2003-01-0581, Detroit.

[14] Chakraborty, N., and Ghosal, A., 2003, "Kinematics of wheeled mobile robots with toroidal wheels on uneven terrain," Proceedings of ASME Design Engineering Technical Conference, Paper No. DETC2003/DAC-48846, Vol. 2B, pp. 1331–1341.

[15] Chakraborty, N., 2003, "Modeling of Wheeled Mobile Robots on Uneven Terrain," M.Sc. thesis, ME Department, Indian Institute of Science, Bangalore, India.

[16] Farritor, S., Hacot, H., and Dubowsky, S., 1998, "Physics-based planning for planetary Exploration," Proceedings of the IEEE ICRA 1998, Leuven, Belgium, pp. 278–283.

[17] Haug, E. J., 1989, *Computer Aided Kinematics and Dynamics of Mechanical Systems*, Allyn and Bacon, Vol. 1.

[18] Montana, D. J., 1988, "The kinematics of contact and grasp," Int. J. Robot. Res., **7**, pp. 17–32.

[19] Wolfram, S., 1999, *The Mathematica Book*, 4th ed., Cambridge University Press, Cambridge.

[20] *ADAMS Users Guide*, MSC Software, USA.

[21] *MATLAB Users Manual*, Mathwork Inc., 1992.